

Electrochemical Corrosion of Ti6Al4V, Ti and AISI 316L SS After Immersed in Concentrated Simulated Body Fluid¹

A. Buyuksagis

Afyon Kocatepe University, Science and Literature Faculty, Afyonkarahisar, Turkey

e-mail: ayselbuyuksagis@hotmail.com, absagis@aku.edu.tr

Received April 6, 2015

Abstract—The biomimetic method is used to obtain hydroxyapatite (HAP) coatings on Ti6Al4V, Ti and AISI 316L SS substrates. These substrates with different pretreatment surface operations (HNO₃, anodic polarization, base-acid) were immersed in concentrated simulated body fluids (SBF) for different days at physiologic conditions of 37°C, initial pH of 7.4. Then the corrosion behaviours of substrates after immersion in concentrated SBF were examined by electrochemical methods in Ringer's and 0.9 wt% NaCl solutions at a temperature of 37°C. Ions concentrations and pH analyses were carried out after incubation in concentrated SBF. After immersion in SBF for different days, the surface morphology remains almost unchanged and no apatite formation is observed. Corrosion currents of substrates increased after immersion. Ions concentrations and pH values were shown variability according to soaking time and pretreatment surface operations.

DOI: 10.1134/S2070205116040067

1. INTRODUCTION

The repair or replacement of damaged hard tissues such as bone is a major clinical problem around the world. Titanium, Ti6Al4V alloy and AISI 316L SS are widely used as orthopedic and dental implant materials due to their low elastic modulus, good biocompatibility and corrosion durability. However, bone does not bond directly to these materials as they get encapsulated by fibrous tissue after implantation, which isolates them from the surrounding bone [1–13]. In order to enhance the bone-bonding ability, titanium, its alloys and AISI 316L SS are often coated with hydroxyapatite (HAP). HAP is known for its biocompatible, bioactive (i.e. ability of forming a direct chemical bond with surrounding tissues), osteoconductive, non-toxic, non-inflammatory, non-immunogenic properties [6, 7, 10, 11, 13–20]. Many different techniques have been used application of HAP coatings onto metal substrates; biomimetic, dip coating, thermal spraying and pulsed laser deposition, electrolytic deposition, electrochemical deposition, a sol-gel method, sputter coating, using wet chemical precipitation methods, hydrothermal treatments, electrodeposition and (micro)emulsion techniques. Most of them were conducted to obtain HAP nanoparticles having ideal stoichiometry and high crystallinity [5, 21–24].

Recent researchs have shown that the biomimetic process is one of the most promising techniques for producing a bioactive coating at ambient temperature

[21–24]. This is a method in which a biologically active apatite layer is formed on a substrate after immersion in an artificially prepared supersaturated calcium and phosphate solution known as SBF [25]. The use more concentrated SBF solution allows the deposition of an homogeneous Ca-P coating within 24 h and a few hours [1, 2, 4, 26–28].

This paper presents, the biomimetic method is used to obtain hydroxyapatite (HAP) coatings on Ti6Al4V, Ti and AISI 316L SS substrates. The solutions are prepared concentrated simulated body fluid (SBF) as 1.5xSBF and 3.0xSBF. Additionally, three different pretreatment surface operations (HNO₃, anodic polarization, base-acid) are applied to the substrates. Substrates soaked in 3.0xSBF and 1.5xSBF solution different immersion periods of 1, 2, 3, 4, 5, 6, 7 days. Corrosion behavior of substrates after immersion were examined in the Ringer's and 0.9 wt % NaCl solutions at a temperature of 37°C. Ions concentrations and pH analyses were carried out after incubation in concentrated simulated body fluid

2. EXPERIMENTAL

2.1. The Preparation of the Substrates

Surface properties of the substrates play a major role in the development of biomimetic HAP coatings and their corrosion resistance. Commercially available Ti6Al4V alloy, pure Ti and AISI 316L SS substrates are used. They are polished with SiC paper at different grades (240, 400, 600, 800, 1000 and 1200), washed by

¹ The article is published in the original.

Special constitutions of SBF, blood plasma, 1.5xSBF and 3.0xSBF

Ions	Na ⁺	K ⁺	Ca ²⁺	Mg ²⁺	Cl ⁻	HCO ₃ ⁻	HPO ₄ ²⁻	SO ₄ ²⁻
SBF concentration (mmol dm ⁻³)	142.00	5.00	2.50	1.50	147.80	4.20	1.00	0.50
Blood plasma concentration (mmol dm ⁻³)	142.00	5.00	2.50	1.50	103.80	27.00	1.00	0.50
1.5xSBF concentration (mmol dm ⁻³)	213.00	7.50	3.75	2.25	221.70	6.30	1.50	0.75
3.0xSBF concentration (mmol dm ⁻³)	426.00	15.00	7.50	4.50	443.40	12.60	3.00	1.50

using Bandelin ultrasonic bath for 15 min in order acetone, alcohol and rinsed with bidistilled water at 30°C and finally dried in an oven at 40°C. Thus, they are made ready for pretreatment surface operations (PTSO).

2.2. Pretreatment Surface Operations of Substrates (PTSO)

Overall the experiments, the chemicals used for the study were reagents grade (Merck) precisely weighted. Three pre-treatments are applied in order to accelerate the coating process, including acid treatment (HNO₃), acid treatment- alkali treatment (BA), and anodic treatment (anodic).

These are summarized as follows:

a) Acid-base (BA) PTSO: The substrates are immersed in 5 mol dm⁻³ NaOH solutions for 12 h at 60°C and they are kept for 12 hours at 25°C. Then, they are washed in the ultrasonic bath for 15 minutes by bidistilled water for two times and are dried oven at 40°C for one hour. After that substrates were kept in 1 mol dm⁻³ HCl at 60°C for 12 h, and then 12 h at 25°C. Following the acid treatment, the substrates are rewashed in the ultrasonic bath for 15 min with bidistilled water for two times and are dried in the drying oven at 40°C for one hour [1, 4, 5, 10, 19, 23, 24, 28–34].

b) Anodic polarization PTSO: Anodic polarization is done in 1 mol dm⁻³ HCl aqueous solution. It is confirmed that optimum treatment time was 300 s in 1 mol dm⁻³ HCl aqueous solution and the potential value is determined as 5 V.

c) HNO₃ PTSO: Substrates were soaked for 20 min in technical HNO₃ and after the acid treatment, the substrates are washed with running bidistilled water and dried at 40°C for one hour. The substrates are cleaned in Bandelin ultrasonic bath for 15 min in order acetone, alcohol, and bidistilled water 30°C. Then, substrates are dried at 40°C for one hour in the drying oven. Surface of substrates is made porous for HAP coating. Substrates are kept in desiccator after put in locked plastic bags [35–39].

2.3. Experimental studies of biomimetic HAP coating

HAP coating with biomimetic method is summarized as follows:

a) The ion concentration in SBF closely resembles the concentration of human blood plasma are prepared using Kokubo's formulation by dissolving reagent-grade of CaCl₂, K₂HPO₄ · 3H₂O, KCl, NaCl, MgCl₂ · H₂O, NaHCO₃ and Na₂SO₄ in bidistilled water. SBF solutions are prepared as 3.0xSBF and 1.5xSBF. Special constitutions of SBF, blood plasma, 1.5xSBF and 3.0xSBF [1, 35–38, 40–42] are given on Table 1. BA, HNO₃ and anodic PTSO are applied separately to substrates. To increase ion concentration and to make easier the composition of the core apatite, solutions are prepared as 1.5xSBF and 3.0xSBF and buffering at physiological pH of 7.4 with 0.1 mol dm⁻³ tris (hydroxymethyl) aminomethane (TRIS) and 0.1 mol dm⁻³ hydrochloric acid (HCl) at 37°C [44]. TRIS was used to provide stability of solution [1, 33, 43–50]. Results described in the literature [43] where SBF is shown to be easily contaminated by bacteria even after short time exposure unless the experiments are conducted under strict aseptic conditions its concentration in the solution. Furthermore, these bacteria can be a health risk for the human [51]. In order to prevent bacterial reproduction NaN₃ was added to the solution as it will be 20 mg dm⁻³ [52, 53].

Prepared concentrated SBF solutions stored in glass bottles and kept in a refrigerator. The SBF shall be used within 30 days after preparation [34]. They could be equilibrated at the testing temperature and carefully mixed just before use [54].

b) 3 samples of substrates are put in each glass bottle. Surface areas of Ti and Ti6Al4V substrates were 2.0096 cm² and totally 75 cm³ concentrated SBF solution is added [33, 35]. For that surface area of AISI 316L SS substrates were 0.785 cm², totally 40 cm³ concentrated SBF is added [35, 44, 55, 56].

c) Glass bottles are put into the the shaking water bath and shaking speed is arranged as 80 rpm, bath temperature 37°C [57]. The substrates are soaked in concentrated SBF for various periods of from 1 to 7 days before they are taken out for testing and analysis. After the biomimetic HAP coating in concentrated SBF solutions, substrates are washed kindly with bidistilled water, kept in the drying oven at 40°C for

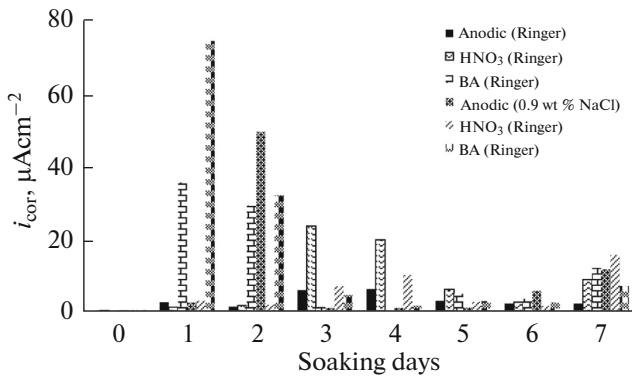


Fig. 1. Corrosion current densities of Ti6Al4V substrates after immersed in 3.0xSBF for different soaking days.

3 h and they are sintered in furnace at 850°C for one hour [39].

d) The ion concentrations in the SBF are measured directly after the samples were removed, using Perkin Elmer Plasma 400 inductively coupled plasma atomic emission spectrometer (ICP-AES). Three readings are taken to obtain the average value [3, 4, 40, 41, 44–49, 57, 58]. At the same time pH values are measured by using ORION pH meter.

e) Corrosion experiments are carried out in 0.9 wt % NaCl and Ringer's solutions. A conventional three-electrode cell is used for all the electrochemical measurements. A saturated calomel electrode (SCE) is used as a reference electrode, platinum foil as a counter electrode and Ti6Al4V, Ti and AISI 316L SS substrates as the working electrodes. All potentials referred to the saturated calomel electrode. Solutions are prepared with bidistilled water using Merck grade reagents. Measurements are obtained using a system consisting of a Reference 600 potentiostat/galvanostat/ZRA system. In order to test the reproducibility of the results, the experiments were repeated three times.

3. DISCUSSIONS

The concentrated SBF solution is not refreshed during the soaking procedure. The results of the SBF soaking test confirm that apatite cannot form on the surface of substrates [24]. Uchida et al. [59] reported that anatase and rutile may provide atomic arrangements in their crystal structures suitable for the epitaxy of apatite crystals. The apatite formation on rutile TiO₂ takes longer immersion time [30]. After reaching their critical size, seeds can start growing into crystals. The nucleation and growth kinetics of the crystal depend on the temperature, pH, composition, and saturation of the solution. Calcium and phosphate ions are responsible for the formation of the calcium phosphate layer on the metal surface [5]. Figure 1 shows corrosion current densities of Ti6Al4V substrates after immersed in 3xSBF for different soaking

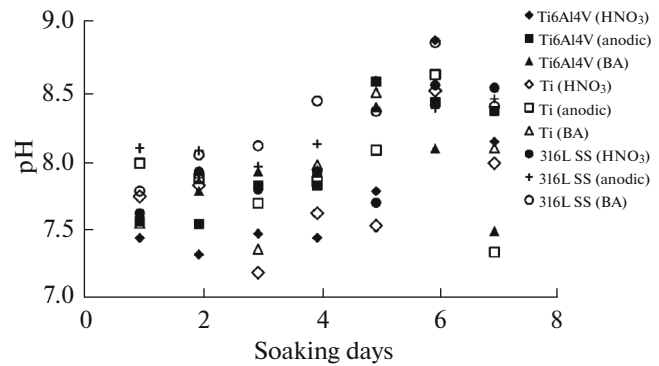


Fig. 2. pH values of substrates after immersed in 3.0xSBF for different soaking days.

time periods E_{corr} values of HNO₃ and anodic PTSO Ti6Al4V substrates in Ringer's solution (immersion in 3xSBF) shifted to more positive potentials. Hydroxyapatite coating with biomimetic method in 3xSBF solution did not occur on the surface of Ti6Al4V substrates. Corrosion current densities of Ti6Al4V substrates are the level of μA although 3xSBF solution (about 3 times concentrated than body fluid) is very intensive. Corrosion resistance of Ti6Al4V are very low, β_a and β_c values can be changeable according to solution type (0.9 wt % NaCl and Ringer's solution) and soaking times. Krupa et al. [46] study have shown that after the oxidation of titanium, the corrosion resistance increases. After long-term exposures, calcium phosphates were found on the sample surface, and their amount was bigger on the oxidised surfaces. As a result of corrosion experiments of Ti6Al4V substrates are carried out in Ringer's solution (HNO₃ PTSO and immersed in 3xSBF), corrosion current density is increased with increasing duration time until 3rd days. Ti6Al4V alloy in 0.9 wt % NaCl solution shows same behavior despite being a few exceptions. Corrosion currents in 0.9 wt % NaCl are less than Ringer's solution in 3rd, 4th, 5th days of soaking. pH values of substrates after immersed in 3.0xSBF for different soaking days is given Fig. 2. Considering pH change for HNO₃ PTSO Ti6Al4V substrates (Fig. 2), pH is increased as the immersion time increases in concentrated SBF solution. This shows that apatite nucleation starts on surface consist of oxides and hydroxides. Ca²⁺ ions increased until 5th holding days (except 4th holding days) then they decreased (Fig. 3).

This indicates that Ca²⁺ ions are solved in a SBF solution [23]. CaO phase is formed Ca²⁺ in hydroxyapatite structure more readily soluble and Ca²⁺ concentrations were varied anodic and BA PTSO Ti6Al4V substrates. When the concentration of PO₄³⁻ analyzed is decreased till 5th immersion days and then it is increased. This can be interpreted PO₄³⁻ contributed to

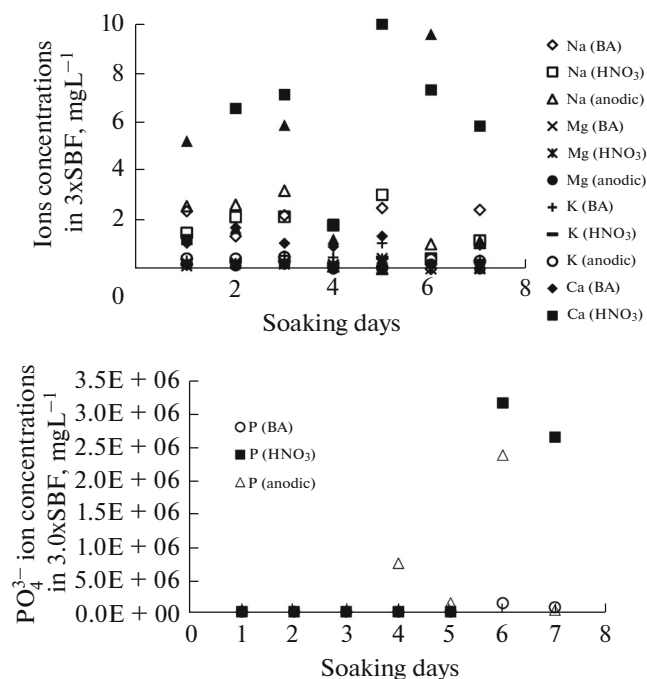


Fig. 3. Ions concentrations after immersed in 3.0xSBF for different soaking days and Ti6Al4V.

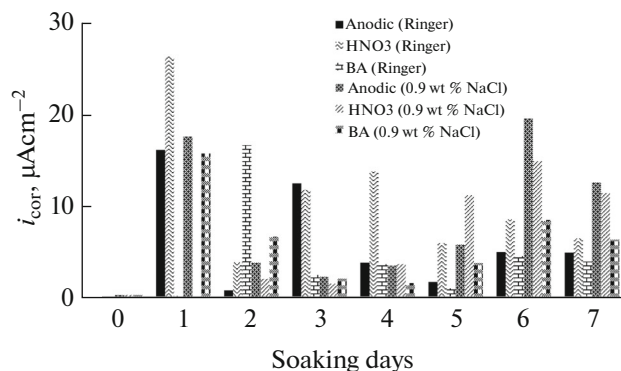


Fig. 4. Corrosion current densities of Ti substrates after immersed in 3.0xSBF for different soaking days.

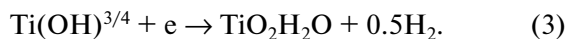
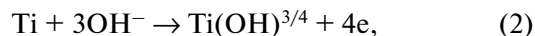
the formation of apatite on the surface of Ti6Al4V substrates and then 5th soaking days apatite rapidly dissolved in SBF solution. Consequently corrosion experiments of Ti6Al4V substrates in Ringer's solution (immersed in 3xSBF and anodic PTSO), corrosion current density is increased until 4th days of exposure to concentrated SBF solution (excepts 2nd days). This shows that corrosion products occurred on the of the Ti6Al4V substrate cover of surface, therefore the corrosion current densities are decreased. Corrosion experiments of the Ti6Al4V substrate in 0.9 wt % NaCl solutions (anodic PTSO and soaked in 3xSBF), corrosion current densities are increased until 4th day of

immersion (except 2nd days) then corrosion current densities increased. TiO₂ can be occurred on the surface of Ti6Al4V substrates by using anodic PTSO with potentiostat this product will help to passivation of surface. pH is increased as the immersion time increased (Fig. 2). Ca²⁺ ions concentration shows variability according to conditions. Increase of Ca²⁺ ions in solution according to ICP-OES analysis shows that Ca²⁺ ions soluble from the surface of substrat (Fig. 3). It can be interpreted decrease of Ca²⁺ ions in solution supported apatite formation. The same thing can be said of phosphate ions.

When we considering corrosion experiments of Ti6Al4V in Ringer's solution (soaked in 3xSBF and BA PTSO substrates). Although corrosion current density increases in the first days of immersion and then decreases gradually again in the next 4th days. Corrosion current densities of Ti6Al4V after 5th and 6th soaking in 3xSBF have not increased notably and 7th days significantly increased.

The formation and growing of apatite on Ti implant surface support by alkali PTSO and then heat treatment process [60]. A porous layer after alkaline PTSO is occurred. During drying process come cracks comprise. Cracks are caused by the thermal coefficients are due to the difference between the metal and hydroxyapatite [60]. The cracks are sourced by the diffusion reaction between the coated surface and SBF. Some micro cracks is by virtue of diffusion of ions from SBF to coating surface. The ions solubility in hydroxyapatite coating are affected from phase crystallinity porosity and thick of metal substrate [23]. pH changes of substrates (BA PTSO and immersed in 3xSBF) increased until 5th soaking days (Fig. 2) then decreased pH increase is supported the apatite formation [5].

The NaOH pre-treated titanium metal forms apatite in a biological environment through the following mechanism. The metal releases sodium ions from the surface amorphous sodium titanate layer into the surrounding fluid through an ion exchange process and with the hydronium ions present in the surrounding fluid leads to form Ti-OH groups on its surface. The Ti-OH groups induce apatite nucleation, and the released sodium ions accelerate the apatite formation by increasing the pH of the fluid.



Corrosion current densities of Ti substrates after immersed in 3.0xSBF for different soaking days is given Fig. 4.

When Fig. 4 is noted that corrosion current density of pure Ti in 0.9 wt % NaCl solution (soaked in 3xSBF and HNO₃ PTSO) is very small. Percent inhibition value is 99%. The corrosion experiments in Ringer's

solution (soaked in 3.0xSBF and HNO₃ PTSO) corrosion current densities show variability depending on immersion time. In this instance surface of Ti consisted of oxides and hydroxides. Grown out of oxide and hydroxides covered the surface of Ti caused decrease of corrosion current density. Acid etching of titanium generates a TiH₂ layer and subsequent NaOH treatment induces the growth of a sodium titanate layer. Immediately after exposure of pre-treated titanium to SBF, calcium and hydronium ions substitute sodium that is leached from the sodium titanate layer. The formation of OH⁻ groups at the surface leads to pH increase and thus to an increase of the ionic activity and of the super saturation of the SBF solution with respect to carbonated apatite in the region near the surface. As a result a calcium phosphate nucleates on the calcium titanate layer [61].

In addition, after the soaking experiments, sintering process is performed in a muffle furnace. Sintering process is carried out 850°C for one hour by use normal air. Titanium at high temperature is very sensitive to H₂, O₂ and N₂ gases and occur titanium oxide and titanium nitride oxidized by these gases. Titanium hydride rapidly develops upper 250°C. Absorption of O₂, N₂ and H₂ leads to fragility at high temperatures [62]. When short duration time experiments (1–7 days) are analyzed in 3xSBF solution, corrosion currents are seen higher (excepts some exception). Likewise, pH values (Fig. 2) are variable of corrosion current densities. Naturally or anodically formed oxide on Ti, which essentially consists of Ti dioxide (TiO₂), effectively protects the metal from rapid dissolution in the harsh body environment. Furthermore, the oxide film enables Ti to exhibit bioactivity in body fluid by providing a site for the deposition of calcium and phosphate compounds and thus induce ionic exchange with apatite from bone tissue [6]. It is important that the anodized surfaces, where the oxide layer was intentionally increased, interacted more actively with modified SBF. Anodized surfaces have more oxygen, a higher chemical potential (*e.g.*, OH⁻), and Ca²⁺ and P³⁻ ions incorporated during anodic oxidation [63].

In Figs. 5 and 6 summarized different biomimetic conditions used to produce apatite coating, also from the first day until 7th days of immersion, corrosion current densities of hydroxyapatite coated 316 L stainless steel are increased and polarization resistance of them are decreased. i_{corr} values of 316L SS are considerably higher than Ti6Al4V alloy and Ti substrates. According to Nagayama and Kawamura [64]; the film layer on the iron are as follows: They founded that outer layer Fe₂O₃ formed in the active zone consist of Fe₃O₄ on the iron surface.

Studies on retrieved implants showed that more than 90% of the failure of 316L SS-implants is due to localized electrochemical cells resulting in pitting attack, or crevice corrosion at the interface between a

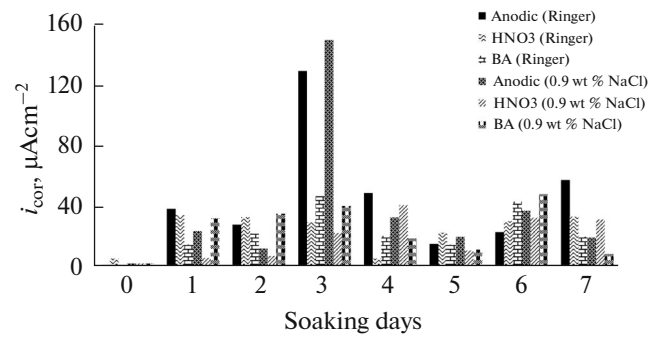


Fig. 5. Corrosion current densities of AISI 316L SS substrates after immersed in 3.0xSBF for different soaking days.

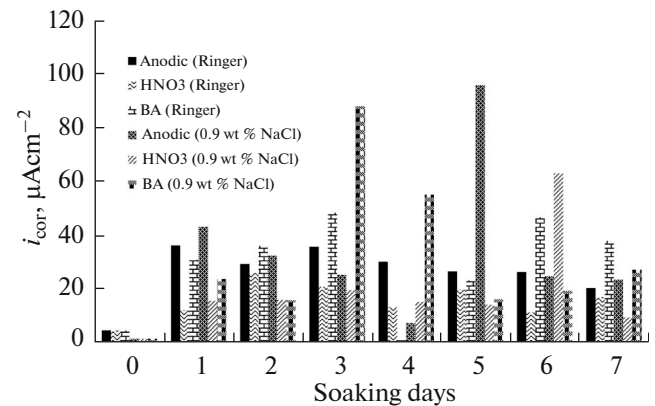


Fig. 6. Corrosion current densities of AISI 316L SS substrates after immersed in 1.5xSBF for different soaking days.

plate and a locking screw. The increased electrochemical activity by increasing the deformation degree might be related to the increased martensite content due to deformation. The martensite phase could act as an anode in an electrochemical cell and is thereby prone to selective dissolution. Chloride ions are adsorbed preferentially on martensite locations and then react with the surface film. This leads to destruction of the surface film and delays its restoration. Generally, corrosion resistance of stainless steels is achieved by dissolving a sufficient amount of chromium in iron to produce a coherent, adherent, insulating and regenerating chromium oxide protective film (Cr₂O₃) on the surface. This passive film of chromium oxide formed in air at room temperature is only about 1–2 nm. Pitting corrosion is the result of the local destruction of the passive film and subsequent corrosion of the steel underneath this layer. The pit formation is influenced by many factors such as martensite content, dislocation density and internal stresses [65]. A. Barbucci et al. [66] have related the pit initiation to the passive film stability, which is influenced by cold deformation. The increased number of pits by increased cold work suggests a much higher defective oxide film in deformed material. Practically

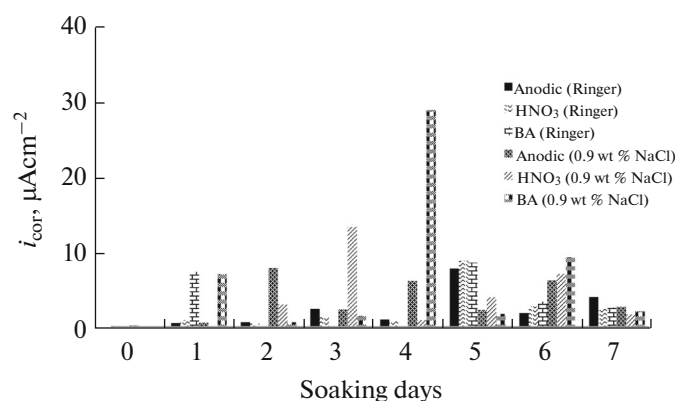


Fig. 7. Corrosion current densities of Ti6Al4V substrates after immersed in 1.5xSBF for different soaking days.

said that Cl^- ions often cause pitting corrosion of metals. The mechanism of pitting corrosion by Cl^- ions is not fully explained. The best explanation for pitting corrosion has been to give the free acids, Cl^- formed HCl to connection water.

Figure 7 presents, corrosion current densities of Ti6Al4V substrates in Ringer's solution (BA PTSO and soaked in 1.5xSBF) are decreased and polarization resistance values are increased 2nd, 3rd, 4th immersed days. Percent inhibition values are calculated for the first day duration time is 66%, for 2nd and 4th days duration time are 90%, for 3rd days duration time is 91%. When metals treated in NaOH are soaked in SBF, the alkali ion in the alkali titanate layer exchanges with the hydronium ion in the fluid, to increase the ionic activity product of the apatite in the fluid by increasing pH. Simultaneously, hydrated titania is formed on their surfaces, and induces the apatite [7]. There aren't any linear change as a result of after corrosion experiments in Ringer's solution (immersed in 1.5xSBF and HNO_3 PTSO). After corrosion experiments in Ringer's solution (soaked 1.5xSBF and HNO_3 PTSO) corrosion current density decreased increasing soaking time till 2nd days and increased 3rd

and 5th duration time days. Lu et al. [67] proposed that the increased surface roughness of the Ti specimen by etching with mixed acids led to good adherence between Ca-P coatings and substrates.

Hereby corrosion experiments in 0.9 wt % NaCl solution (immersed in 1.5xSBF and HNO_3 PTSO), corrosion current density of Ti6Al4V substrates increased until 3rd days of immersion and then variability show increase and decrease. When we look at pH changes (Fig. 8), HNO_3 PTSO Ti6Al4V substrates), they are seen that the formation of oxide on Ti6Al4V surface ions quantity of Ca^{2+} ions (Fig. 9 and HNO_3 PTSO) are decreased (except 5th days duration time). Decreasing Ca^{2+} ions in solutions show that Ca^{2+} ions deposited on the substrates for formed apatite. In solution analysis phosphate quantity is decreased. This show that formation of apatite less than 3xSBF avoided and a uniform surface coverage of apatite on the Ti6Al4V substrates was obtained according to the following equation [5].



Cationic species, i.e. Ca^{2+} and Mg^{2+} are favorably attracted onto the TiO_2 passive layer covering Ti6Al4V plates. Titanium substrate is believed to be negatively charged at physiological pH, whereas results show evidences for chemical affinities between Ti and HPO_4^{2-} but rarely Ti and Ca^{2+} [2]. The negatively charged surfaces are always favorable for the heterogeneous nucleation of HAP in a supersaturated solution called "simulated body fluid" (SBF) or Kokubo solution, whereas the nucleation is inhibited on positive surfaces. The accepted interpretation is that the accumulation of Ca^{2+} ions due to the electrostatic attraction increases the super saturation near the negative surfaces, and as a result, the initial nucleation is preferentially triggered [34].

The presence of Na^+ , HPO_4^{2-} , HCO_3^- , Ca^{2+} , Cl^- in the aqueous media of SBF maintained at 7.4 pH results in formation of NaCl; increased ionic strength

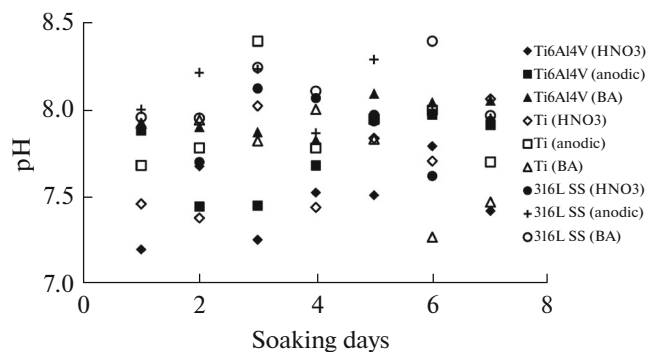


Fig. 8. pH values of substrates after immersed in 1.5xSBF for different soaking days.

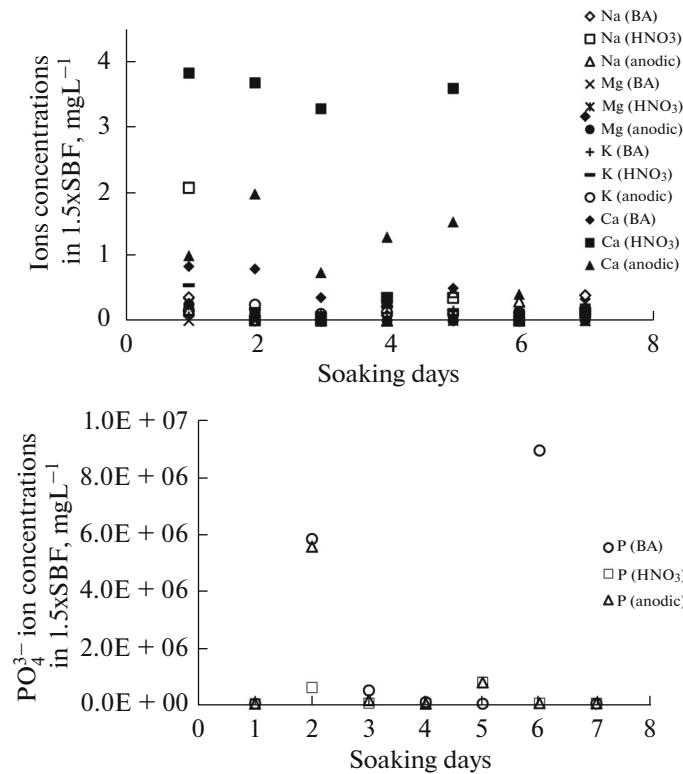


Fig. 9. Ions concentrations after immersed in 1.5xSBF for different soaking days and Ti6Al4V.

leads to an increase in pH of solution [69]. The as-deposited thin films soaked in SBF for 4 weeks did not show any notable amount of apatite particles on their surfaces [70].

Corrosion current densities of Ti6Al4V substrates in Ringer's solution (soaked in 1.5xSBF and BA PTSO) are very low 2nd, 3rd and 4th days of exposure to 1.5xSBF solution, Ti6Al4V alloy shows the passivity properties. Then corrosion increased breakdown of passive film. Corrosion current densities of Ti6Al4V substrates in 0.9 wt % NaCl solution (soaked in 1.5xSBF and BA PTSO) is decreased until 3rd and 4th days of immersion as regional corrosion current is increased by breaking the film. Corrosion current is reduced again to repair film itself. Ca²⁺ ions in solution 6th days of immersion. After NaOH-treatment of the Ti6Al4V substrate, due to surface passivation TiO₂ is formed. The alkali treatment produces negatively charged Ti-O-groups interacting with positively charged Ca²⁺ ions, which in turn attract phosphate ions from the precursor solution to form an initial calcium-phosphate layer [5, 11, 24, 25, 29, 34, 71].

Figure 10 offers, the corrosion current densities are increased, polarization resistance are decreased. Corrosion current densities compared in 0.9 wt % NaCl and Ringer's solution, corrosion current densities of anodic PTSO Ti substrates are lower than corrosion

currents of BA PTSO and HNO₃ PTSO Ti substrates (1st, 2nd, 3rd and 5th days of immersion). Corrosion experiments of Ti substrates (HNO₃ PTSO and immersed in 1.5xSBF) corrosion current densities increase with increasing duration time till 6th days. The chemical treatment with an acidic HNO₃ aqueous solution (pH = 0.7) results in an anatase-type TiO₂ film of very low crystallinity (TiO₂ gel) formed on the Ti surface. The Ti-OH groups reportedly act as nucleation sites for HAP on TiO₂. As pointed out in, the Ti-

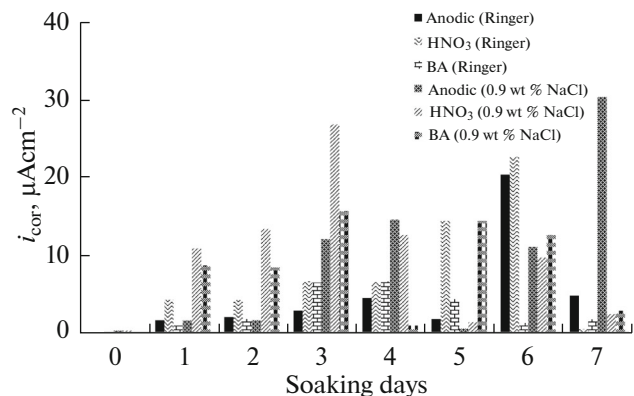


Fig. 10. Corrosion current densities of Ti substrates after immersed in 1.5xSBF for different soaking days.

OH groups react with hydroxyl ions in the SBF, (pH = 7.4), leading to a negatively charged surface with functional Ti–O-groups. The latter attract from the SBF positively charged Ca^{2+} ions which in turn attract negatively charged PO_4^{3-} ions from the solution. Subsequently, a calcium-phosphate layer is formed on the TiO_2 surface. Thus, soaking in H_2O_2 results in the formation of Ti–OH groups owing to the interaction of Ti cations from the oxide layer with OH^- groups in the aqueous medium. The Ti–OH groups may be either acidic or basic, depending on the pH of the solution, hence, higher pH values provide better conditions for the HA nucleation and growth.

Once apatite nuclei are formed, they grow spontaneously by calcium and phosphorous ions from the surrounding solution and this can be further enhanced if the sodium titanate on its surface is converted into anatase Ti [5].

Corrosion current densities of Ti substrates (soaked in 1.5xSBF and HNO_3 PTSO) are increasing with increased duration time till 3th days of immersion. At this stage oxides and hydroxides formed on Ti surface. Formed these oxides and hydroxides covered the Ti surface and corrosion is reduced.

Corrosion currents of Ti substrates in Ringer's solution (immersed in 1.5xSBF and anodic PTSO) are increased with increasing soaking time until 4th days. At this stage oxides and hydroxides formed on Ti surface. Corrosion current is decreased until 5th and 7th days of immersion, corrosion current increased 6th days of immersion. Similar behaviour is observed in 0.9 wt % NaCl solution. Corrosion currents of Ti substrates in 0.9 wt % NaCl solution (soaked in 1.5xSBF and BA PTSO) changeability demonstrated. Etching in either alkaline or acid solution is often used to obtain Ti-OH bonds and porous structures to induce HAP deposition [6]. It is suggested that a porous network of the titanium surface arising after the NaOH pretreatment favors the nucleation of calcium phosphates [11].

First of all corrosion current densities decreased then resulting oxides and hydroxides surface closed. Corrosion currents increased due to aggressive chloride ions in the Ringer's and 0.9 wt % NaCl solution. The measured pH values (Fig. 8, BA PTSO Ti) is typically considered to be 7.28 and above. The cathodic reaction in neutral and alkaline solutions are in the form of reduction of water and oxygen. For this reason at these pH's formed oxides and hydroxides on the surface. Aforementioned explains increasing and then decreasing the corrosion is due to oxides and hydroxides formation.

It should also be emphasized that the modification of SBF had reproducible and effective results on biomimetic deposition. A limitation of biomimetic deposition is the slow rate of CaP deposition, with a lack of

reproducibility of its effects due to the arbitrary SBF composition [54].

4. CONCLUSIONS

- Apatite cannot form on the surface of substrates after concentrated SBF soaking tests.
- pH is increased as the immersion time increases in concentrated SBF solutions
- Increase of Ca^{2+} and PO_4^{3-} ions in concentrated SBF solution shows that ions soluble from the surface of substrates
- Corrosion current densities increased with duration soaking times.

ACKNOWLEDGMENTS

The author gratefully acknowledge the Scientific and Technical Research Council of Turkey (TUBITAK) for the financial support with the Grant Number of 107M563.

REFERENCES

1. Bharati, S., Sinha, M., and Basu, D., *Bull. Mater. Sci.*, 2005, vol. 28, p. 617.
2. Barrere, F., van Blitterswijk, C., de Groot, K., and Layrolle, P., *Biomaterials*, 2002, vol. 23, p. 2211.
3. Barriere, F., Layrolle, P., van Blitterswijk, C., et al., *Bone*, 1999, vol. 25, p. 107S.
4. Bigi, A., Boanini, E., Bracci Facchini, A., et al., *Biomaterials*, 2005, vol. 26, p. 4085.
5. Faure, J., Balamurugan, A., Benhayoune, H., et al., *Mater. Sci. Eng.: C*, 2009, vol. 29, p. 1252.
6. Anawati Tanigawa, H., Asoh, H., Ohno, T., et al., *Corros. Sci.*, 2013, vol. 70, p. 212.
7. Janković, A., Eraković, S., Mitrić, M., et al., *J. Alloys Compd.*, 2014, vol. 624, p. 148.
8. Mohseni, E., Zalnezhad, E., and Bushroa, A., *Int. J. Adhes. Adhes.*, 2014, vol. 48, p. 238.
9. Pasinli, A., Yuksel, M., Celik, E., et al., *Acta Biomater.*, 2010, vol. 6, p. 2282.
10. Stoch, A., Jastrzebski, W., Brozek, A., et al., *J. Mol. Struct.*, 2000, vol. 555, p. 375.
11. Yanovska, A., Kuznetsov, V., Stanislavov, A., et al., *Surf. Coat. Technol.*, 2011, vol. 205, p. 5324.
12. Yoon Il-Kyu, Hwang Ji-Young, Jang Won-Cheoul, et al., *Appl. Surf. Sci.*, 2014, vol. 301, p. 401.
13. Sutha, S., Kavitha, K., Karunakaran, G., and Rajendran, V., *Mater. Sci. Eng.: C*, 2013, vol. 33, p. 4046.
14. Swetha, M., Sahithi, K., Moorthi, A., et al., *Int. J. Biol. Macromol.*, 2010, vol. 47, p. 1.
15. Cai, Q., Feng, Q., Liu, H., and Yang, X., *Mater. Lett.*, 2013, vol. 91, p. 275.
16. McLeod, K., Kumar, S., Dutta, N.K., et al., *Appl. Surf. Sci.*, 2010, vol. 256, p. 7178.
17. Minh, D.P., Nzihou, A., and Sharrock, P., *Mater. Res. Bull.*, 2014, vol. 60, p. 292.

18. Mohseni, E., Zalnezhad, E., and Bushroa, A.R., *Int. J. Adhes. Adhes.*, 2014, vol. 48, p. 238.
19. Sadjadi, M.S., Meskinfam, M., Sadeghi, B., et al., *Mater. Chem. Phys.*, 2010, vol. 124, p. 217.
20. Štulajterova, R. and Medvecký, L., *Colloids Surf., A*, 2008, vol. 316, p. 104.
21. Hashizume, M., Nagasawa, Y., Suzuki, T., et al., *Colloids Surf., B*, 2011, vol. 84, p. 545.
22. Gao, F., Xu, C., Hu, H., et al., *Mater. Lett.*, 2015, vol. 138, p. 25.
23. Gu, Y.W., Khor, K.A., and Cheang, P., *Biomaterials*, 2003, vol. 24, p. 1603.
24. Chu, C.L., Pu, Y.P., Yin, L.H., et al., *Mater. Lett.*, 2006, vol. 60, p. 3002.
25. Zhang, Q. and Leng, Y., *Biomaterials*, 2005, vol. 26, p. 3853.
26. Costa, D.O., Allo, B.A., Klassen, R., et al., *Langmuir*, 2012, vol. 28, p. 3871.
27. Čolović, B., Jokanović, V., Jokanović, B., and Jović, N., *Ceram. Int.*, 2014, vol. 40, p. 6949.
28. Habibovic, P., Barrère, F., van Blitterswijk, C.A., et al., *J. Am. Ceram. Soc.*, 2002, vol. 85, p. 517.
29. Chen, X., Li, Y., Hodgson, P.D., and Wen, C., *Mater. Sci. Eng.: C*, 2009, vol. 29, p. 165.
30. Gu, Y.W., Tay, B.Y., Lim, C.S., and Yong, M.S., *Biomaterials*, 2005, vol. 26, p. 6916.
31. Jalota, S., Bhaduri, S.B., and Tas, A.C., *Mater. Sci. Eng.: C*, 2008, vol. 28, p. 129.
32. Holzwarth, J.M. and Ma, P.X., *Biomaterials*, 2011, vol. 32, p. 9622.
33. Tas, A.C., *J. Eur. Ceram. Soc.*, 2000, vol. 20, p. 2389.
34. Kokubo, T. and Takadama, H., *Biomaterials*, 2006, vol. 27, p. 2907.
35. Jonasova, L., Muüller, F.A., Helebrant, A., et al., *Biomaterials*, 2004, vol. 25, p. 1187.
36. Khor, K.A., Li, H., Cheang, P., and Boey, S.Y., *Biomaterials*, 2003, vol. 24, p. 723.
37. Saiz, E., Goldman, M., Gomez-Vega, J.M., et al., *Biomaterials*, 2002, vol. 23, p. 3749.
38. Ning, C.Q. and Zhou, Y., *Biomaterials*, 2002, vol. 23, p. 2909.
39. Büyüksağis, A., Çiftci, N., Ergün, Y., and Kayalı, Y., *Prot. Met. Phys. Chem. Surf.*, 2011, vol. 47, p. 670.
40. Lin, C.M. and Yen, S.K., *Mater. Sci. Eng.: C*, 2006, vol. 26, p. 54.
41. Wei, D. and Zhou, Y., *Ceram. Int.*, 2009, vol. 35, p. 2343.
42. Forsgren, J., Svahn, F., Jarmar, T., and Engqvist, H., *Acta Biomater.*, 2007, vol. 3, p. 980.
43. Ciobanu, G., Carja, G., and Ciobanu, O., *Surf. Coat. Technol.*, 2008, vol. 202, p. 2467.
44. Lluch, A.V., Ferrer, G.G., and Pradas, M.M., *Colloids Surf., B*, 2009, vol. 70, p. 218.
45. Kannan, S., Balamurugan, A., and Rajeswari, S., *Electrochim. Acta*, 2004, vol. 49, p. 2395.
46. Krupa, D., Baszkiewicz, J., Sobczak, J.W., et al., *J. Mater. Process. Technol.*, 2003, vol. 144, p. 158.
47. Balamurugan, A., Balossier, G., Kannan, S., et al., *Ceram. Int.*, 2007, vol. 33, p. 605.
48. Ding, S.J., Huang, T.H., and Kao, C.T., *Surf. Coat. Technol.*, 2003, vol. 165, p. 248.
49. Rigo, E.C.S., Boschi, A.O., Yoshimoto, M., et al., *Mater. Sci. Eng.: C*, 2004, vol. 24, p. 647.
50. Jalota, S., Bhaduri, S., and Tas, A., *Mater. Sci. Eng.: C*, 2007, vol. 27, p. 432.
51. Müller, L. and Müller, F., *Acta Biomater.*, 2006, vol. 2, p. 181.
52. Xiao, X.F., Tian, T., Liu, R.F., and She, H., *Mater. Chem. Phys.*, 2007, vol. 106, p. 27.
53. Shi, Y., Downes, M., Xie, W., et al., *Genes Dev.*, 2001, vol. 15, p. 1140.
54. Bohner, M. and Lemaitre, J., *Biomaterials*, 2009, vol. 30, p. 2175.
55. Oliveira, A.L., Costa, S.A., Sousa, R.A., and Reis, R.L., *Acta Biomater.*, 2009, vol. 5, p. 1626.
56. Sánchez-Salcedo, S., Balas, F., Izquierdo-Barba, I., and Vallet-Regí, M., *Acta Biomater.*, 2009, vol. 5, p. 2738.
57. Li, F., Feng, Q.L., Cui, F.Z., et al., *Surf. Coat. Technol.*, 2002, vol. 154, p. 88.
58. Chou, Y.F., Chiou, W.A., Xu, Y., et al., *Biomaterials*, 2004, vol. 25, p. 5323.
59. Uchida, M., Kim, H.M., Kokubo, T., et al., *J. Biomed. Mater. Res., Part A*, 2003, vol. 64, p. 164.
60. Escada, A.L.A., Rodrigues, D., and Machado, J.P.B., *Surf. Coat. Technol.*, 2010, vol. 205, p. 383.
61. Müller, F.A., Müller, L., Caillard, D., and Conforto, E., *J. Cryst. Growth*, 2007, vol. 304, p. 464.
62. Şengil, İ.A., Korozyon, İ.T.Ü. *Sakarya Mühendislik Fakültesi Matbaası*, 1992, vol. 1501, p. 494.
63. Sul, Y.T., Johansson, C.B., Petronis, S., et al., *Biomaterials*, 2002, vol. 23, p. 491.
64. Nagayama, M. and Kawamura, S., *Electrochim. Acta*, 1967, vol. 12, p. 1109.
65. Mhaede, M., Ahmed, A., Wollmann, M., and Wagner, L., *Mater. Sci. Eng.: C*, 2015, vol. 50, p. 24.
66. Barbucci, A., Delucchi, M., Panizza, M., et al., *J. Alloys Compd.*, 2001, vols. 317–318, p. 607.
67. Lu, X., Zhao, Z., and Leng, Y., *Mater. Sci. Eng.: C*, 2007, vol. 27, p. 70.
68. Kokubo, T., *Thermochim. Acta*, 1996, vols. 280–281, p. 479.
69. Karanjai, M., Sundaresan, R., Mohan, T.R.R., and Kashyap, B.P., *Mater. Sci. Eng.: C*, 2008, vol. 28, p. 1401.
70. Amin, M.S., Randeniya, L.K., Bendavid, A., et al., *Diamond Relat. Mater.*, 2012, vol. 21, p. 42.
71. Chi, M.H., Tsou, H.K., Chung, C.J., and He, J.L., *Thin Solid Films*, 2013, vol. 549, p. 98.